Intermediate-structure fusion resonances observed in the radiative capture of ^{12}C by ^{12}C

A. M. Nathan
University of Illinois at Urbana-Champaign, Urbana, Illinois 61801

A. M. Sandorfi
Brookhaven National Laboratory, Upton, New York 11973

T. J. Bowles*
Argonne National Laboratory, Argonne, Illinois 60439

(Received 3 April 1981)

We have investigated the $^{12}C(^{12}C,\gamma)^{24}Mg$ reaction, populating low-lying states of ^{24}Mg, with $^{12}C + ^{12}C$ c.m. energies between 5 and 11 MeV. High energy γ rays were detected in a large volume NaI spectrometer which had sufficient resolution to distinguish clearly the γ_0, γ_1, and $\gamma_{2,3}$ transitions. Several resonances were observed in each of the decay channels. In particular, the γ_0 excitation function has four narrow resonances at $E_{c.m.} = 5.6$, 6.0, 6.8, and 8.0 MeV, which are unambiguously assigned $J^\pi = 2^+$. The upper three of these resonances are correlated in all three decay channels but are not correlated either with previously identified 2^+ structures in the $^{12}C + ^{12}C$ system or with structure in the distribution of ground-state $E2$ strength in ^{24}Mg. Furthermore, calculations demonstrate that these resonances have large nonstatistical ^{12}C- and photon-partial widths. We argue that the data are suggestive of a new and unusual form of intermediate structure, namely highly clustered $^{12}C + ^{12}C$ configurations built on the ground-state band of ^{24}Mg.

[NUCLEAR REACTIONS $^{12}C(^{12}C,\gamma)^{24}Mg$, $5 \leq E_{c.m.} \leq 11$ MeV; measured $E\gamma$, $d\sigma/d\Omega(45°, E\gamma_0)$, $d\sigma/d\Omega(45°, E\gamma_1)$, $d\sigma/d\Omega(45°, E\gamma_{2,3})$; deduced Γ, Γ_γ $\Gamma_{^{12}C}/\Gamma$, and $E_{c.m.}$ for isolated resonances.]

I. INTRODUCTION

The study of resonances in light heavy-ion systems has long been a topic of interest in nuclear physics. This is especially true of the $^{12}C + ^{12}C$ system,[1] which is rich in resonances ranging from below the Coulomb barrier to $E_{c.m.} \simeq 40$ MeV and in spin from 0^+ up to perhaps as high as 18^+. These resonances have been discussed in the framework of the doorway state formalism of Feshbach, Kerman, and Lemmer.[2] In this treatment the gross structure ($\Gamma \gtrsim 1$ MeV) is described as the strong coupling of the entrance channel to a shape resonance in the $^{12}C + ^{12}C$ interion potential, while the finer structure ($\Gamma \lesssim 0.3$ MeV) results from the coupling of this doorway state to more complicated intermediate states.[3] Various authors differ on their description of the intermediate states and how they couple to the shape resonances.[4-6] Experimentally these states are generally characterized by large decay widths into the $^{12}C + ^{12}C$ entrance channel ($\Gamma_c/\Gamma \gtrsim 0.1$ from whence comes the designation "quasimolecular"), while the decay probabilities into other channels are more or less consistent with a statistical evaporation from the compound nucleus. There are exceptions, of course, and authors have attempted to associate enhanced decay probabilities in various channels with particular models for the intermediate structure.[4-6]

One decay channel that has received little systematic attention, either theoretical or experimental, is the photon decay of these $^{12}C + ^{12}C$ structures to low-lying levels of ^{24}Mg. If, for example, it could be demonstrated that a particular resonance has an enhanced γ-decay probability to the ^{24}Mg ground state, then this would signal an unusual type of intermediate structure that not only has an appreciable overlap with the $^{12}C + ^{12}C$ entrance channel, but is also simply connected to the fused nucleus through a single-particle operator. The first experimental suggestion that such unusual states exist arose from an observation by Sandorfi *et al.*,[7] of a narrow anomaly at an excitation energy $E_x \approx 22$ MeV in the electrofission of ^{24}Mg into two ^{12}C nuclei in their ground states, although this anomaly did not correspond to any previously known features of $^{12}C + ^{12}C$ reactions. Subsequently, the inverse $^{12}C(^{12}C,\gamma_0)^{24}Mg$ radiative capture reaction was investigated.[8] The narrow resonance was confirmed and preliminary values for its width and capture strength were reported. Furthermore, although the data were somewhat sparse, it was apparent that other resonances existed between $E_{c.m.} = 6$ and 8 MeV in both the γ_0 and γ_1 decay channels. However, it was still uncertain if any of the previously identified quasimolecular resonances γ decayed to ^{24}Mg or whether resonances appearing in the radiative-capture yields reflected some new type of inter-

mediate structure. In the present paper, we report on an extension of these capture measurements in which we have searched for resonances in the $^{12}C(^{12}C,\gamma)^{24}Mg$ reaction in the $E_{c.m.}=5-11$ MeV range with an experiment designed to resolve as many γ-decay channels as possible. In Sec. II we describe our experimental setup and data reduction technique. An analysis of the data is presented in Sec. III, in which we deduce parameters for the observed resonances, compare the data with known structure in the $^{12}C+^{12}C$ and in the $E2$ strength functions, and attempt to account for the data with a statistical calculation. Based on this analysis, we attempt to interpret the data in terms of the nature of the intermediate structure (Sec. IV). The conclusions are summarized in Sec. V. Preliminary accounts of various aspects of this work have appeared elsewhere.[8-11]

II. EXPERIMENTAL METHOD AND DATA REDUCTION

The data we will discuss in the subsequent sections were taken in three separate experiments extending over three years. The first experiment (BNL No. 1), which was performed at the Brookhaven National Laboratory MP6 Tandem Van de Graaff and was reported in our earlier publication (Ref. 8), covered the energy range from 5.0–11.0 MeV (c.m.), with targets varying in thickness from 0.3–0.6 MeV c.m. The second experiment, which was performed at the Argonne National Laboratory (ANL) FN Tandem, covered the entire energy range from 5.6–8.8 MeV with an average target thickness of 0.3 MeV. The third set of data were taken at MP6 again (BNL No. 2) and carefully covered the range from 5.3–6.2 MeV as well as scattered points at higher energies, all with a thin ($\lesssim 0.2$ MeV) target. Except for the fact that the energy resolution in the photon detector was considerably worse in the first experiment ($\gtrsim 7\%$) than in the other two ($\lesssim 4\%$), the experimental setup and essential parameters were virtually the same for all three data runs. Therefore, in order to simplify the following discussion, we described in detail only the ANL setup.

A schematic drawing of the setup is shown in Fig. 1. A 5-cm diam thin-walled stainless steel vacuum chamber housed the target and beam stop. The target, a self-supporting foil of ^{13}C-depleted carbon mounted on a Ta ring, was oriented at 68° with respect to the beam axis. The thickness of the foil exposed to the beam, determined by measuring the energy loss of α particles from a ^{241}Am source, was 104 ± 3 $\mu g/cm^2$. This corresponded to energy losses for the incident carbon beam ranging from 675 keV (for $E_{lab}=11.5$ MeV)–550 keV (for $E_{lab}=17.83$ MeV). A Ta collimator located 2.5 cm upstream of the target shadowed the target frame from the beam. The beam was stopped in a Ta strip which lined the rear of the target chamber. Each run was normalized to the total integrated charge (typically 5000 particle-μC) from the beam stop, which included the target but not the collimator. The latter was electrically insulated so that the beam current striking it could be measured (less than 10% of the total) and was maintained at +300 V with respect to the target/beam stop to prevent secondary electrons from the collimator from striking the beam dump. We estimate the absolute accuracy of the current integration to be about 15% and the relative accuracy from run to run to be good to about 5%.

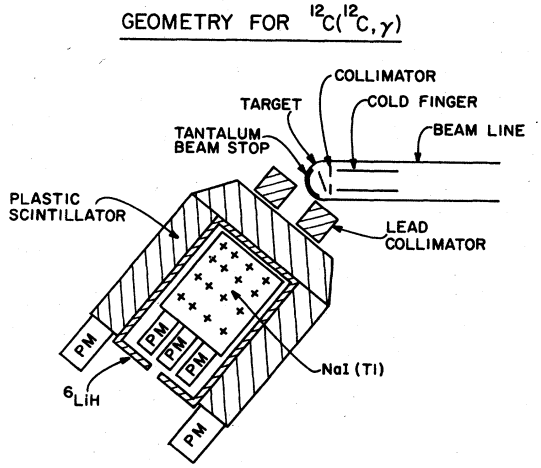

FIG. 1. Schematic drawing of the experimental setup for the $^{12}C(^{12}C,\gamma)^{24}Mg$ experiment.

The vacuum in the target chamber was maintained at about 2×10^{-6} torr (2.6×10^{-4} Pa) throughout the experiment. Carbon buildup on the target and beam stop was reduced to a negligible amount by a 1.3-cm diam by 15 cm long liquid-N_2-cooled tube, through which the beam passed, just before the Ta collimator. No visible traces of carbon deposits were evident on the Ta beam stop after seven consecutive days of rather intense bombardment.

High energy γ rays were detected at 45° in a large NaI(Tl) crystal surrounded by plastic scintillator used in anticoincidence to reject escape radiation (see Fig. 1). In view of the low cross sections expected in this experiment ($\lesssim 50$ nb/sr) and the close separations of low-lying states of ^{24}Mg, it was of crucial importance to be able to detect these γ rays with high efficiency and good resolution. The array of seven 7.5-cm diam photomultiplier tubes operated at negative high voltage provided a fairly uniform photocathode surface as well as an inherent stability against gain

drifts. The detector gain was further dynamically stabilized using a commercial gain-control amplifier to lock onto a reference peak from a temperature-stabilized light-emitting diode which injected light into the crystal. An additional peak from an electronic pulser was used to monitor the rate at which valid high energy events were accidentally rejected by the anticoincidence shield or by pileup-detection circuitry. The remainder of the spectrometer, including the plastic anticoincidence shield, the ^{6}LiH neutron shield, and the pulse processing electronics, are fairly standard,[12] and we only note that, for the low cross sections of interest, the good cosmic ray rejection (~98%) was of particular importance.

At the start of the experiment, the detector resolution was optimized using high energy γ rays from the $^{11}B(p,\gamma)^{12}C$ reaction.[13] For this purpose, a few nA of 6.0-MeV protons were incident upon a thin ^{11}B foil. Since one can choose a proton energy such that the γ_0 and γ_1 peaks bracket the region of interest to the $^{12}C(^{12}C,\gamma)$ experiment, we were able to generate *in situ* the detector response functions for essentially monoenergetic γ rays for use in the data analysis described below. A typical spectrum from $^{11}B(p,\gamma)$ is shown in Fig. 2 where the resolution of the ANL detector is about 3.8% FWHM.

For the $^{12}C+^{12}C$ experiment, the beam current was adjusted at each bombarding energy so that the total counting rate in the NaI was kept at an acceptable level (typically 10^5 sec^{-1} above 1 MeV). For low bombarding energies (e.g., 11.5 MeV which is below the Coulomb barrier), this required essentially the maximum current the accelerator could provide (~1 particle-μA), while at 17.8 MeV, the current was limited to 0.3 particle-μA due to the rapid increase in the total reaction cross section for energies just above the Coulomb barrier. Essentially all the counting rate was due to interactions with the carbon target.

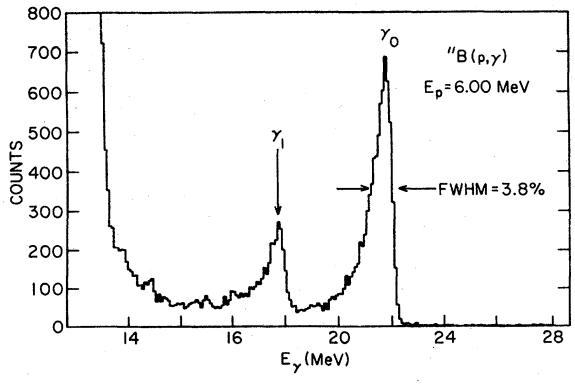

FIG. 2. The ANL-detector response to high energy γ rays from the $^{11}B(p,\gamma)^{12}C$ reaction at E_p=6.0 MeV and θ=45°. The indicated resolution was typical of that achieved during the ANL measurements.

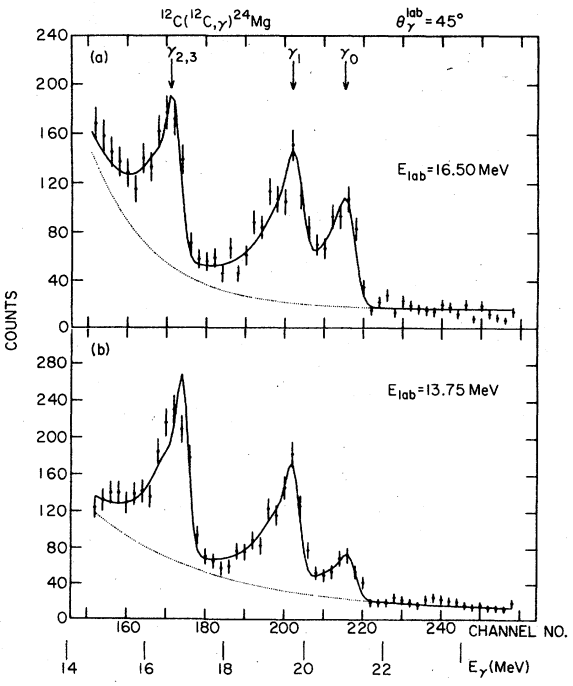

FIG. 3. Typical ANL spectra of high energy γ rays from $^{12}C(^{12}C,\gamma)^{24}Mg$ at 45°. The solid line is the result of a nonlinear least-squares fit to the data, assuming 3 peaks and a smooth background, which is indicated by the dotted line. The spectrum in (a) has been shifted down in energy by 1.38 MeV relative to the spectrum in (b) in order to compare both with the same energy scale.

Typical $^{12}C(^{12}C,\gamma)^{24}Mg$ spectra taken at ANL are shown in Fig. 3. One can clearly identify the γ_0, γ_1, and the unresolved $\gamma_{2,3}$ peaks, corresponding to decays to the ground state, 1.37 MeV 2^+ state, and 4.1–4.2 MeV 4^+–2^+ doublet, respectively. These peaks are superimposed upon a smooth background due primarily to the pileup of many lower energy events (especially γ rays from neutron capture in the NaI). Although the spectra taken at lower bombarding energies clearly show lines corresponding to decays up to the 7th excited state of ^{24}Mg, the pileup of the low energy background in most of the data limited the analyzable transitions to γ_0, γ_1, and $\gamma_{2,3}$.

The response of the detector used in the BNL No. 2 measurements to isolated γ rays from $^{11}B(p,\gamma)$ at Ep=6.00 MeV is shown in Fig. 4(a). The indicated resolution of 3.3% was typical for this set of measurements, and a sample $^{12}C(^{12}C,\gamma)$ spectrum is shown in Fig. 4(b).

The data were analyzed by fitting the spectra to an exponential plus constant background, and three peaks with fixed parametrized shapes chosen to fit the $^{11}B(p,\gamma)$ spectra. Peak positions were allowed to vary in the fit, but in all cases the fitted positions were consistent with those deduced from the known Q value, excitation energies in ^{24}Mg, beam energy, Dopper shift, and the γ-ray energy calibration determined from $^{11}B(p,\gamma)$.

The resulting laboratory-differential cross sections at 45° are shown in Fig. 5 (ANL), Fig. 6 (BNL No. 2), and Fig. 2 of Ref. 8 (BNL No. 1). The vertical error bars include statistical contributions only. For both sets of BNL data, the absolute cross section scale was determined from independent *in situ* measurements of the known $^{11}B(p,\gamma_0)$ cross section.[13] We note that the BNL

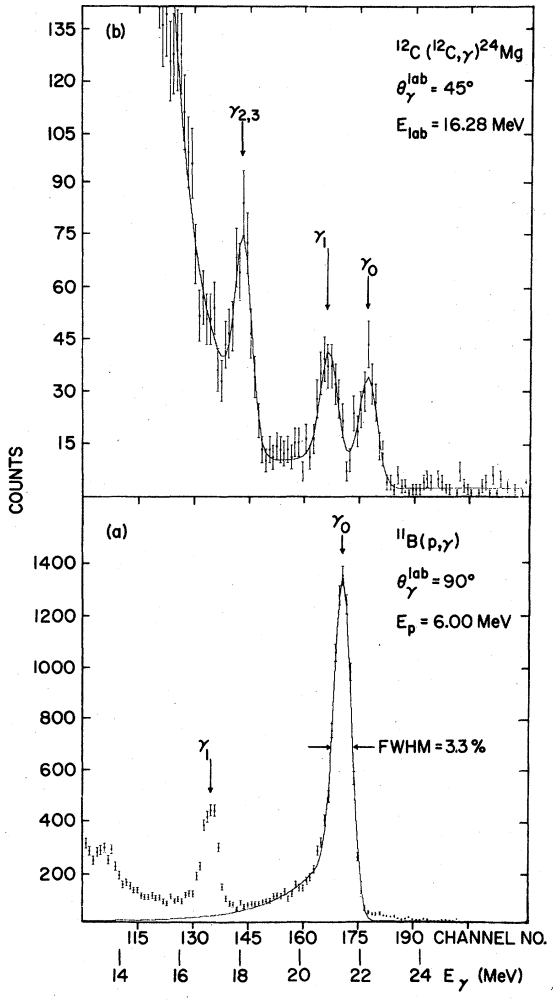

FIG. 4. Response of the detector used in the BNL No. 2 measurements to high energy γ rays from $^{11}B(p,\gamma)^{12}C$ in (a), and from $^{12}C(^{12}C,\gamma)^{24}Mg$ in (b). The solid curve in (a) is the intrinsic line shape for this detector, fitted to the γ_0 peak. See caption to Fig. 3.

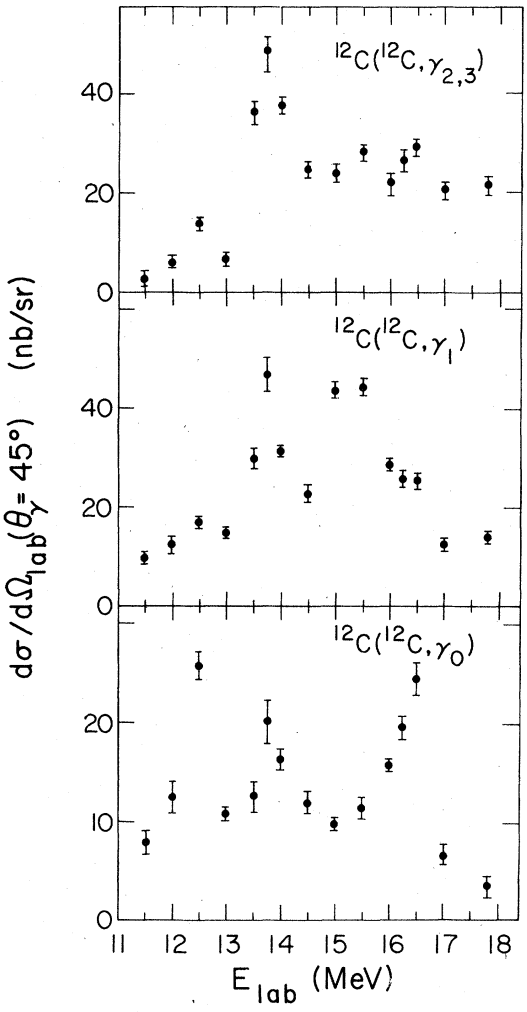

FIG. 5. Excitation functions for $^{12}C(^{12}C,\gamma)^{24}Mg$ at 45° (ANL data). The error bars indicate the statistical uncertainties from the fitting procedure.

No. 1 published cross sections should be lowered by 9% to correct for dead time effects. Since no reliable normalization runs were made at ANL, all those data were adjusted using a *single* normalizing factor to provide the best overlap with the BNL data. All of the data have been converted to c.m.-differential cross sections and are plotted in Fig. 7, where the vertical bars again represent statistical uncertainties only and the horizontal bars represent the c.m. target thickness. [The BNL No. 1 data plotted in Fig. 7 has been renormalized to the latest value of the $^{11}B(p,\gamma_0)$ cross section (Ref. 13). In Ref. 8 the cross section of Ref. 13(a) had been used.] The dashed line through the γ_0 data represents the results of a fit described below, while the lines through the γ_1, and $\gamma_{2,3}$ data are only to guide the eye. The good agreement among the several data sets for γ_0 and γ_1 gives us

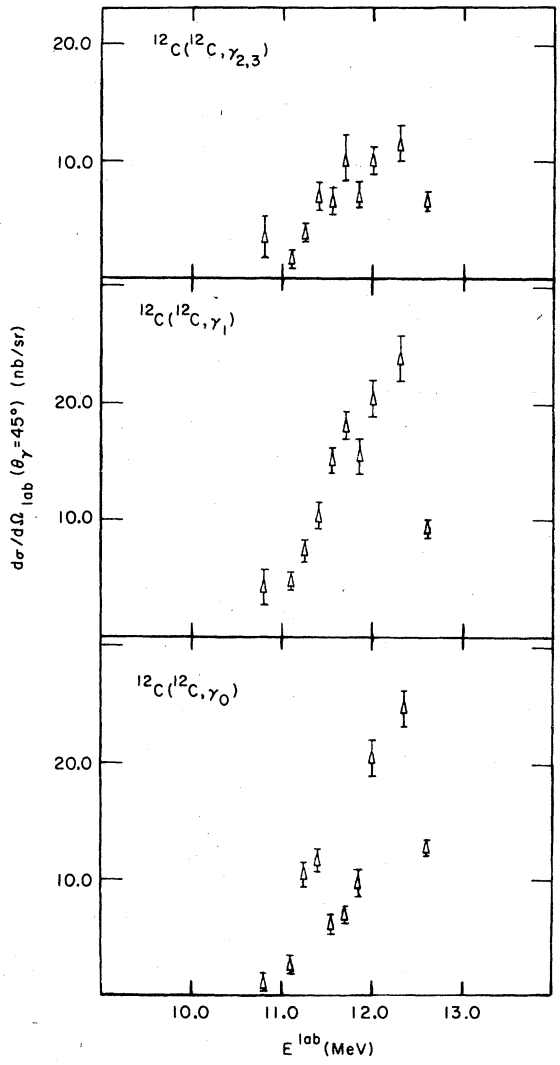

FIG. 6. Excitation functions for $^{12}C(^{12}C,\gamma)^{24}Mg$ at 45° (BNL No. 2 data). Only those data at $E_{lab}<13$ MeV are shown. (Five remaining points from this data set, taken at scattered higher energies, are included in Fig. 7.) The error bars represent statistical uncertainties.

confidence that our normalization procedure is reasonable. The few discrepancies, we believe, are largely associated with the BNL No. 1 data in which γ_0 and γ_1 were not clearly resolved. In particular, the high point in the γ_0 yield curve near $E_{c.m.}=8$ MeV is correlated with a low point in γ_1—the summed γ_0 and γ_1 cross sections at that energy agree with the subsequent better resolution data. The same seems to be true of the low point in γ_0 near 7.2 MeV. We point this out mainly because it changes our perspective of the γ_0 resonance near 8 MeV ($E_x\simeq 22$ MeV in ^{24}Mg) which we now believe to be somewhat broader than reported in Ref. 8 (see discussion below). For $\gamma_{2,3}$ the discrepancies are somewhat larger and we attribute these to systematic effects associated with the subtraction of the steep background under the $\gamma_{2,3}$ peak (see Figs. 3 and 4).

III. DATA ANALYSIS

There are two striking features of the $^{12}C(^{12}C,\gamma)$ excitation functions that are immediately apparent. First, the yield is localized, especially in the γ_0 channel, extending from about 5.5–8.5 MeV c.m. Outside this region the cross section is greatly diminished. Second, within that gross structure, there is considerable finer structure in the form of narrow ($\Gamma\lesssim 0.3$ MeV) resonances, several of which appear correlated in all three γ-decay channels. In this section we first examine possible correlations between these resonances and previously identified structures in both the entrance ($^{12}C+^{12}C$) and exit (γ) channels. To this end, we have performed a multiresonance fit to the capture data in order to extract values for the resonance energies, total widths, and capture strengths (Sec. III A). In Sec. III B, we compare these results to previously identified 2^+ and 4^+ quasimolecular resonances. In Sec. III C, we look for correlations between the γ_0 data and the best available data for the $E2$ photoabsorption cross section. And finally, in Sec. III D we investigate whether the capture data can be accounted for by the mechanism of compound nucleus formation followed by competitive statistical decay. The results of this section form the basis for the discussion of Sec. IV.

A. Multiresonance fit to the γ_0 data

In order to at least semiquantitatively parametrize the capture data, we have fitted the γ_0 excitation function to an incoherent sum of five Breit-Wigner resonances. These represent the four obvious resonances in Fig. 7(a) plus a fifth broad bump at ~9.2 MeV with a width of ~2 MeV that approximates a smooth background under the lower energy peaks. There is no real justification for neglecting interference effects except that the resonances appear well separated in energy; in any case, we would have no guidance whatsoever as to the relative phases. The expression used in the fit was

$$\frac{d\sigma}{d\Omega}(\theta,E)=2\left[\frac{15}{32\pi}\sin^2(2\theta)\right]\pi\lambda^2(2J+1)\sum_{i=1}^{5}\frac{\Gamma_{\gamma_i}\Gamma^0_{c_i}}{\Delta E}\int_{E-\frac{\Delta E}{2}}^{E+\frac{\Delta E}{2}}\frac{T(E')dE'}{(E'-E_i)^2+\Gamma_i^2/4}. \quad (1)$$

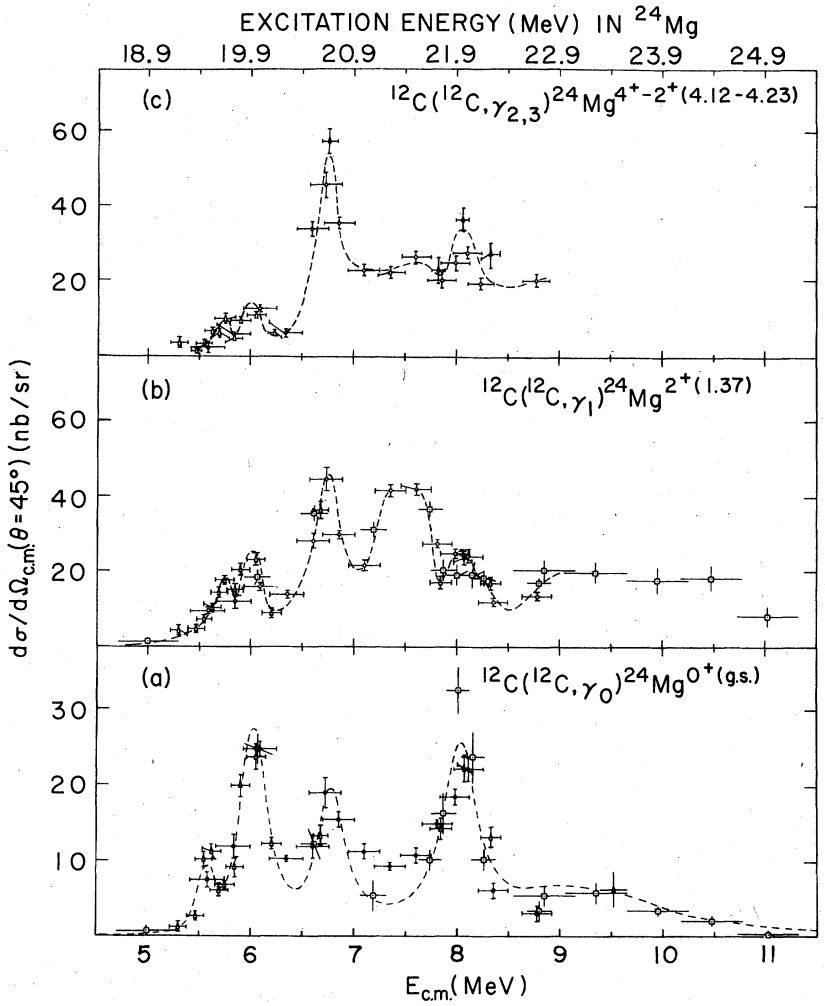

FIG. 7. Excitation functions for ^{12}C(^{12}C,γ)^{24}Mg at 45° plotted against $\langle E_{c.m.}\rangle$, the c.m. energy at the center of the target. The corresponding excitation energy scale is given at the top of the figure. Vertical bars indicate statistical uncertainties in the cross section whereas horizontal bars indicate the c.m. energy loss in the target. Data from all three experiments are shown: squares are from BNL No. 1, circles from ANL, and triangles from BNL No. 2. The dashed line for γ_0 is the result of a least-squares fit to a sum of Breit-Wigner resonances, while the lines for γ_1 and $\gamma_{2,3}$ are merely to guide the eye and suggest possible correlation.

The initial factor of 2 is included because there are identical particles in the entrance channel. Further, we note that $\frac{15}{32}\pi \int \sin^2(2\theta)d\Omega = 1$, $\lambda\!\!\!^{-}$ is the reduced wavelength in the c.m., and ΔE is the c.m. target thickness. Also E_i, Γ_i, and Γ_{γ_i} are the c.m. energy, total width, and ground-state radiative width of the ith resonance, while $\Gamma^0_{c_i}$ is the "intrinsic" carbon width and $T(E)$ is the ^{12}C + ^{12}C transmission coefficient ($0 \leq T \leq 1$). The latter factor was included to account for changes in the ^{12}C escape probability over the width of the resonance, so that the *observed* carbon width of the resonance Γ_{c_i} is given by $\Gamma^0_{c_i}\, T(E_i)$. The T's were calculated using the optical-model code PTOLEMY (Ref. 14) and the optical potential of Ref. 15. Finally, we note that the above formula implicitly assumes quadrupole multipolarity ($J=2$). For identical bosons in the entrance channel, J^π is restricted to 0^+, 2^+, 4^+, ..., while observation of a decay photon to the 0^+ ground state rules out 0^+ and makes multipolarities greater than 2 extremely unlikely.[16] Thus $J^\pi = 2^+$ for all resonances observed in the γ_0 channel. Similarly, resonances observed in γ_1 [$J_f^\pi = 2^+$] are effectively restricted to 0^+, 2^+, or 4^+.

In the fitting procedure, E_i, Γ_i, and the quantity $\Gamma^0_{c_i}\Gamma_{\gamma_i}/\Gamma_i$ were allowed to vary for each of the five resonances, except for the lowest resonance

for which the width was constrained to its previously determined value of 0.130 MeV,[17] (see discussion in Sec. III B). Two points from the poorer-resolution BNL No. 1 data were excluded from the least-squares fit, namely the high point at 8.0 MeV and the low point near 7.2 MeV (see previous section). The results are presented in Table I and the cross section, given by Eq. (1) using the fitted-resonance parameters and assuming a fixed target thickness of $\Delta E = 0.200$ MeV, is plotted as the dashed curve in Fig. 7(a). The parametrization of Eq. (1) appears adequate for most of the γ_0 excitation function. The fit falls below the data near 6.4 and 7.4 MeV, which may indicate contributions from additional less-prominent structures (see discussion in Sec. III D). Different parametrizations of the background in the γ_0 excitation function are of course possible. These can change the strengths ($\Gamma^0_{c_i}\Gamma_{\gamma_i}/\Gamma_i$) of the prominent resonances appreciably, but have relatively little effect on peak positions (E_i) and widths (Γ_i).

B. Comparisons with known $^{12}C+^{12}C$ resonances

In Fig. 8 the γ_0 excitation function [8(b) solid curve] is compared with the positions of previously[17-21] identified $^{12}C+^{12}C$ 2^+ resonances [8(c) and Table II]. We believe the γ_0 peak near 5.6 MeV corresponds to the 2^+ resonance at 5.63 MeV with $\Gamma = 0.130$ MeV and $\Gamma_c = 0.010$ MeV. The peaks at 6.0 and 8.0 MeV do not seem to correlate with any $^{12}C+^{12}C$ 2^+ structures. [The 6-MeV bump may, however, coincide with a 2^+ peak reported in $^{20}Ne(\alpha,\gamma_0)^{24}Mg$.[22]] Finally, the γ_0 peak near 6.8 MeV is close to but considerably wider than the 2^+ resonance at 6.64 MeV (with $\Gamma = 0.1$ MeV), so although a contribution to the γ_0 peak from this resonance cannot be ruled out, some significant fraction must be due to a hitherto unreported structure. The main point we are making is that there are definite 2^+ structures apparent in the γ_0 decay channel that have not been previously identified as 2^+ resonances in the $^{12}C+^{12}C$ system.

In Fig. 9 the γ_1 [9(a)] and $\gamma_{2,3}$ [9(d)] excitation functions are compared to the known $^{12}C+^{12}C$ 2^+ [9(b)] and 4^+ [9(c)] resonances (see Table II).[17-21] The 5.6-MeV-γ_0 resonance seems not to be present in these decay channels. The structures seen near 6.0, 6.8, and 8.0 MeV correlate with 2^+ resonances observed in the γ_0-decay channel. However, $4^+ - ^{12}C+^{12}C$ resonances which fall near the same energies may contribute to these peaks in γ_1 and $\gamma_{2,3}$. On the other hand, the 4^+ structures near these energies may contain contributions from 2^+ resonances. For example, a recent analysis of the region near 8 MeV c.m. in $^{12}C(^{12}C,^{16}O)^8Be$ is consistent with both 4^+ and 2^+ components.[23] The peak at 5.75 MeV, present in both γ_1 and $\gamma_{2,3}$, and the broad bump at 7.5 MeV in γ_1 do not correspond in position or width with any of the previously identified structures listed in Table II. Their apparent absence in the γ_0 yield may indicate dominant 4^+ or 0^+ components. (Monopole states in ^{24}Mg that decay into two ^{12}C nuclei have been reported at excitation energies near the region of the 7.5 MeV-γ_1 peak.[7])

C. Comparisons with the $E2$ strength function

The best available data on the distribution of $E2$ strength built on the ^{24}Mg ground state come from several high energy $^{24}Mg(\alpha,\alpha')$ experiments.[24,25] The procedure and the problems involved in deducing $B(E2)$ values from the (α,α') cross sections have been discussed in a recent review by van der Woude.[26] The decomposition of the average $E2$ strength, deduced from high resolution 120-MeV (α,α') data,[25] into a sum of Gaus-

TABLE I. Resonance parameters extracted by fitting the $^{12}C(^{12}C,\gamma_0)^{24}Mg$ excitation function to Eq. (1). Uncertainties are in parentheses.

$E_{c.m.}$ (MeV)	Centroid	E_x (MeV)	Γ (MeV)	$\Gamma^0_c\Gamma_\gamma/\Gamma$ (eV)	$\Gamma_c\Gamma_\gamma/\Gamma^{(a)}$ (eV)
5.56	(0.05)	19.49	0.130[b]	0.154(0.027)	0.011(0.002)
6.01	(0.02)	19.94	0.245(0.042)	0.620(0.050)	0.084(0.007)
6.77	(0.03)	20.70	0.250(0.050)	0.208(0.025)	0.058(0.007)
8.02	(0.02)	21.95	0.342(0.082)	0.141(0.018)	0.090(0.012)
9.17	(0.50)	23.10	2.0(0.6)	0.17(0.03)	0.17(0.03)

[a] This *observed* strength is obtained by multiplying the fitted "intrinsic strength" $\Gamma^0_c\Gamma_\gamma/\Gamma$ by the transmission coefficient $T(E)$ evaluated at the resonance energy.

[b] Constrained to the results of Ref. 17. The value of the centroid of this resonance is slightly smaller than the value given in Ref. 17 (5.63 MeV) due to the rapidly changing transmission coefficient as one crosses the Coulomb barrier—this effect was not considered in Ref. 17.

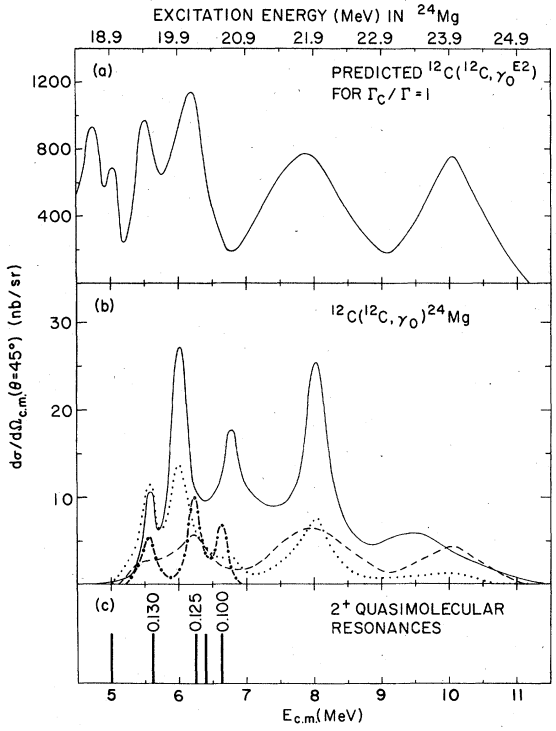

FIG. 8. (a) Predicted capture cross sections for $\Gamma_c/\Gamma = 1$. This curve represents structure in the cross section due to the photon channel alone. (b) The $^{12}C(^{12}C,\gamma_0)^{24}Mg$ excitation function and various calculations. The solid line is a smooth curve *through the* γ_0 *data* shown in Fig. 7(a) [rather than the fit of 7(a)]. The dashed line is the calculation assuming statistical carbon widths. The dotted curve is the prediction assuming the resonant carbon widths in Table I and statistical photon widths. The circle-dashed curve is the prediction for the 3 quasimolecular 2^+ states with known ^{12}C widths in Table II, assuming statistical photon decay. (c) Location of 2^+ quasimolecular states (Table II). Total widths of resonances are indicated in MeV.

sian peaks is given in Table III. The parameter $(\beta R)^2$ is proportional to the area under each peak and is related to the $E2$ radiative width Γ_γ by

$$\Gamma_\gamma = \frac{3}{500\pi}(eZR)^2\left(\frac{E_x^5}{\hbar c}\right)(\beta R)^2, \qquad (2a)$$

or, for ^{24}Mg, taking 3.46 fm for the nuclear radius R

$$\Gamma_\gamma(eV) = (1.59\times10^{-5})E_x^5(\beta R)^2, \qquad (2b)$$

where E_x is the excitation energy in MeV and the deformation length (βR) is in fm. At each energy, we have computed the $E2$ radiative width per MeV, $d\Gamma_\gamma/dE_x$, assuming $d(\beta R)^2/dE_x$ is distributed as the sum of the Gaussian peaks listed in Table III. The $^{12}C(^{12}C,\gamma_0)$ cross section at an excitation energy E_x in ^{24}Mg is related to $d\Gamma_\gamma/dE_x$ by

TABLE II. Previously reported 2^+ and 4^+ $^{12}C+^{12}C$ resonances between 5.0 and 11.0 MeV c.m. (The reference given is not necessarily the primary reference.)

$E_{c.m.}$ (MeV)	E_x (MeV)	J^π	Γ_{TOTAL} (MeV)	Γ_c (MeV)	Γ_c/Γ	Reference
5.00	18.933	2^+				18
5.63	19.563	2^+	0.130	0.010	0.08	19
5.98	19.913	4^+	0.100	0.003	0.03	19
6.26	20.193	2^+	0.125	0.016	0.13	20
6.41	20.343	2^+				21
6.64	20.573	2^+	0.100	0.029	0.29	19
6.83	20.763	4^+	0.125	0.008	0.06	19
7.71	21.643	4^+	0.125	0.022	0.18	20
7.90	21.833	4^+				20
8.10	22.033	4^+				21
8.26	22.193	4^+	0.175	0.039	0.22	20
8.46	22.393	4^+				20
8.58	22.513	4^+				21

$$\frac{d\sigma^{45^\circ}}{d\Omega}(E_x) = 2\left(\frac{25\pi}{64m_0c^2}\right)\frac{(\hbar c)^2}{(E_x-Q)}\frac{\Gamma_c}{\Gamma}\frac{d\Gamma_\gamma}{dE_x}, \qquad (3a)$$

where m_0c^2 and Q are the nucleon mass (931.48 MeV) and Q value (13.93 MeV), respectively. The initial factor of 2 arises from the identity of the incoming particles in the capture reaction. For E_x in MeV and $d\Gamma_\gamma/dE_x$ in eV MeV^{-1} the γ_0 cross section in nb/sr becomes

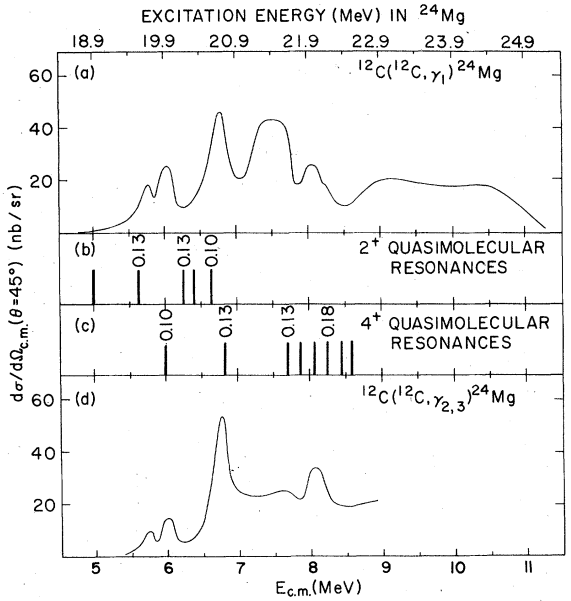

FIG. 9. (a) The $^{12}C(^{12}C,\gamma_1)$ excitation function. (b) Location of 2^+ quasimolecular states (Table II). Total widths of resonances are indicated in MeV. (c) Location of 4^+ quasimolecular states (Table II). Total widths of resonances are indicated in MeV. (d) The $^{12}C(^{12}C,\gamma_{2,3})$ excitation function.

TABLE III. Distribution of $E2$ strength in ^{24}Mg between 14 and 24 MeV as deduced from an analysis of the ^{24}Mg (α,α') reaction (K. van der Borg—Ref. 25).

E_x[a] (MeV)	Width[a] (MeV)	$(\beta R)^2$[b] (fm^2)
14.47	0.170	0.040
14.74	0.170	0.048
16.53	0.140	0.020
16.90	0.490	0.078
17.36	0.220	0.073
17.75	0.250	0.032
18.00	0.350	0.026
18.30	0.280	0.023
18.68	0.280	0.040
19.03	0.210	0.020
19.50	0.350	0.044
19.85	0.280	0.014
20.20	0.490	0.068
21.80	1.410	0.116
24.00	1.060	0.068

[a] Centroid (E_x) and FWHM of a Gaussian.
[b] Area of Gaussian distribution—see Eq. (2) of text.

$$\frac{d\sigma^{45^\circ}}{d\Omega}(E_x)=\frac{1026}{E_x-13.93}\frac{\Gamma_c}{\Gamma}\frac{d\Gamma_\gamma}{dE_x}\,. \tag{3b}$$

So far the treatment is exact, assuming the validity of the functions $d\Gamma_\gamma/dE_x$. If one has a model for Γ_c/Γ, one can use Eq. (3) to directly compare the predictions of that model to the capture data. We have computed and plotted in Fig. 8(a) the right-hand side of Eq. (3) under the condition $\Gamma_c/\Gamma=1$. Thus any structure in the resulting cross section must be due to structure in the photon channel. Upon comparing Fig. 8(a) with Fig. 8(b) solid curve, we see that the 5.6 MeV resonance seems to be correlated with a peak in the $E2$ strength function and the 8.0 MeV resonance is observed near the middle of a much broader structure. However, the 6.0- and 6.8-MeV resonances line up with valleys in the $E2$ distribution. On the whole, the pronounced features of the capture yields do not directly reflect structure in the photon channel.

Finally, we note that since the $E2$ strength functions built upon excited states of ^{24}Mg are not available, we cannot do a similar analysis for γ_1 and $\gamma_{2,3}$.

D. Statistical interpretations of the data

We now wish to examine whether one can interpret the radiative capture data as a process of compound nucleus formation followed by competitive statistical decay. In this description of nuclear reactions, the nucleus is excited in the entrance channel, evolves into complicated compound nuclear states, and subsequently decays in a statistical manner independent of its mode of formation.[27] Following the theory of compound nuclear reactions, the average ^{12}C(^{12}C,γ_0) cross section can be written[28] as

$$\frac{d\sigma^{45^\circ}}{d\Omega}(E_x)=\frac{1026}{E_x-13.93}\frac{(\overline{\Gamma_c/D})(\overline{\Gamma_\gamma/D})}{(\overline{\Gamma/D})}\ \text{nb/sr}\,, \tag{4}$$

where E_x is in MeV, $\overline{\Gamma_c}$, $\overline{\Gamma_\gamma}$, and $\overline{\Gamma}$ are the average carbon, $E2$, and total widths of the underlying 2^+ compound nuclear levels, and D is the average energy interval between those levels. In writing Eq. (4), it has been assumed that there are sufficient numbers of overlapping levels ($\Gamma/D\gg1$) and that the decay amplitudes in the entrance and exit channels are sufficiently uncorrelated, so that the relative phase between these decay amplitudes is essentially random.[28]

In our calculations, we have taken the $E2$ strength function $\overline{\Gamma_\gamma/D}$ to be equal to the values of $d\Gamma_\gamma/dE_x$ deduced from the (α,α') experiment via Eq. (2), Also, we have computed $\overline{\Gamma/D}$ according to the Hauser-Feshbach prescription[27]

$$\overline{\Gamma/D}=\frac{1}{2\pi}\sum_\kappa T_\kappa\,, \tag{5}$$

where T_κ is the optical model transmission coefficient in channel κ and the sum runs over all open channels. We have used the code STATIS (Ref. 29) to compute $\overline{\Gamma/D}$. The optical potential for the alpha-, proton-, neutron-, and ^{12}C-decay channels were taken from Refs. 30–32 and 15, respectively, and discrete levels[33,34] were used up to 14.44, 5.53, 3.80, and 4.44 MeV excitation for final states in the outgoing nuclei, respectively. At higher excitation energies, level densities from Ref. 35 were used. Pairing energies were taken from Ref. 36. In the region of the radiative capture resonances the calculated values for $\overline{\Gamma/D}$ ranged from about 3.2 at 19 MeV excitation in ^{24}Mg to 17.5 at 23 MeV excitation.

We have used two extreme models for the carbon strength function $\overline{\Gamma_c/D}$. First we assume that the carbon widths are nonresonant and essentially the average widths one obtains from a statistical picture. That is,

$$\overline{\Gamma_c/D}=\frac{T_{cc}}{2\pi}\,, \tag{6}$$

where T_{cc} is the ^{12}C+^{12}C transmission coefficient. The point of view here is that a photon excites the nucleus, which then mixes into the compound levels and decays statistically. Using the ^{12}C+^{12}C optical potential of Ref. 15, we have computed capture cross sections in this model, and they are plotted as the dashed line of Fig. 8(b). We see that over most of the range shown, the cal-

culation falls well below the data and accounts for essentially none of the fine structure. It does succeed, however, in explaining the drop in cross section below 5.5 MeV as the result of the Coulomb barrier reduction of T_{cc}. The drop in cross section above 11 MeV may result from a general decrease in Γ_γ, although little is known about the $E2$-strength function at higher energies. In any case, a general decrease in the cross section at higher energies is expected, due to an increase in the number of open channels. Nonetheless, the overall conclusion from this calculation is that the $^{12}C+^{12}C$ partial widths for the resonances seen in radiative capture are significantly enhanced over statistical widths. We next assume that the carbon widths have only resonant components so that

$$\overline{\Gamma_c/D}=\frac{1}{2\pi}\,\frac{\Gamma^2}{(E-E_0)^2+\Gamma^2/4}\,\frac{\Gamma_c}{\Gamma}\ . \tag{7}$$

Here E_0, Γ_c, and Γ are the positions, carbon widths, and total widths of the γ_0 resonances. Our viewpoint now is that a resonance, excited in the $^{12}C+^{12}C$ channel, mixes into the underlying compound levels and emits a photon by virtue of the $E2$ strength of these underlying levels (i.e., the photon decay is statistical). To calculate cross sections under these assumptions, we use the fitted resonance parameters for E_0 and Γ in Table I, and we make a reasonable assumption about Γ_c/Γ. We assume $\Gamma_c/\Gamma=0.14$ (the average for the resonances of Table II) for all but the 5.63-MeV resonance, for which the measured value $\Gamma_c/\Gamma=0.077$ (Ref. 17) is used, and we average over an 0.2-MeV interval to simulate typical target thickness in the data. The result is shown as the dotted curve in Fig. 8(b). The γ_0 decay of the 5.63-MeV resonance is completely consistent with statistical photon emission. The predicted magnitude of the 6.0-MeV resonance is about a factor of 2 below the data and a statistical calculation could account for this peak if Γ_c/Γ were as large as 0.30. However, this would be grossly inconsistent with elastic scattering measurements[19] which have assigned $J^\pi=4^+$, $\Gamma=0.100$ MeV, and a much smaller carbon width $\Gamma_c/\Gamma=0.03$ to the only observed peak near this energy (5.98 MeV—see Table II). The other peaks in the γ_0 yield are far above these predictions. Thus we conclude that, for the most part, the photon widths of the capture resonances are also significantly enhanced over statistical widths.

Finally, we note that the quasimolecular state at 6.26 MeV is not apparent in the capture data, despite the fact that it coincides in excitation energy with a large enhancement in the $E2$ strength function. We can use the formalism described above to ask what would be the contribution of this and the other 2^+ quasimolecular resonances in Table II to the capture cross section under the assumption of compound nucleus formation followed by statistical γ decay. The results for those resonances with known ^{12}C widths are shown as the circle-dashed line in Fig. 8(b), and we conclude that the apparent absence of a peak at 6.26 MeV in the capture data is consistent with the assumption of only a statistical γ decay for this resonance. In fact, such a contribution from the *molecular* resonances at 6.26, 6.41, and 6.64 MeV (Table II) could account for the apparent excess γ_0 yield above the fitted excitation function [dashed curve of Fig. 7(a)] between 6.2 and 6.6 MeV.

IV. DISCUSSION

There are two conclusions to be drawn from the statistical analysis of the preceding section. First, at least one and possibly all of the previously identified quasimolecular resonances (Table II) are present in the radiative capture yields, but only at a very low level consistent with a statistical γ decay. Second, the $^{12}C+^{12}C$ and the γ_0-decay probabilities of the dominant resonances observed in radiative capture are significantly greater than statistical probabilities for capture from the compound nucleus. In addition, the average width of a $J^\pi=2^+$ compound-nuclear level in ^{24}Mg is about 20 keV in the region of these structures, and peaks due to the random coherence in amplitude and phase of strongly-overlapping levels cannot be significantly broader than about 50 keV. Since the total widths of the γ_0 resonances are considerably larger, an Ericson fluctuation phenomenon[37] can be ruled out. We, therefore, conclude that we are observing correlations between the $E2$ and the $^{12}C+^{12}C$ 2^+ strength functions, arising from an unusual form of intermediate structure that is strongly coupled to both the $^{12}C+^{12}C$ fusion channel and the low-lying states of ^{24}Mg. This represents the first clear evidence for a close link between states with large $^{12}C+^{12}C$ parentage and the structure of ^{24}Mg. Furthermore, it is interesting that those states that exhibit this close connection form a new set of resonances which, although undoubtedly present in $^{12}C+^{12}C$ elastic scattering at some level due to their nonstatistical ^{12}C widths, certainly do not correspond to the dominant quasimolecular features seen in $^{12}C+^{12}C$ reactions. That this *new* set of capture resonances has a structure distinct from previously observed resonances may be evident in their γ-decay branches. The 2^+ peaks at 6.0, 6.8, and 8.0 MeV seem to be present in the γ_1 and $\gamma_{2,3}$ excitation functions as well as in γ_0. This is consistent with a close link to the structure of the fused nucleus. The wave functions of the levels in the ground-state

rotational band (GSB) of ^{24}Mg are very similar, and thus 2^+ levels that decay strongly to the ground state would also be expected to have significant decay branches to the 2^+ and 4^+ members of the GSB. In contrast, the *old* 5.6 MeV quasimolecular resonance appears only in the γ_0 excitation function. However, we have argued that the γ decay of this resonance arises from statistical photon emission from an overlapping peak in the distribution of ground-state-$E2$ strength. The $E2$ strength functions built on excited states of ^{24}Mg may be very different, and thus γ decay to the ground state via statistical photon emission need not necessarily imply a comparable decay rate to other members of the GSB.

It is interesting to speculate on the nature of the connection between the structure of ^{24}Mg and the $^{12}C+^{12}C$ system. It may be that the resonances we observe are part of a quadrupole vibration [either a β surface vibration or giant quadrupole (GQR) oscillation] in which the deformed ^{24}Mg ground state is further dynamically distorted to a point of instability, resulting in symmetric fission. However, such a mechanism would require large structural variations across the $E2$ strength distribution, which bears little resemblance to the $^{12}C(^{12}C,\gamma_0)$ excitation function. There has recently appeared in the literature an attempt to link the $K=0$ piece of the GQR in ^{24}Mg (calculated in a 2-centered shell model) to the $^{12}C+^{12}C$ fusion channel.[38] Quantitative predictions for the capture reaction were made, but these fail to account for even the gross features of our data. At present, the unusual structures observed in $^{12}C+^{12}C$ radiative capture remain an interesting puzzle.

V. SUMMARY

We have measured the $^{12}C(^{12}C,\gamma)^{24}$Mg cross section between 5–11 MeV c.m. and have identified several previously unreported resonances. These represent a new and unusual form of intermediate structure in that there are correlated enhancements both in the $^{12}C+^{12}C$ and in the $E2$ photonuclear channels.

ACKNOWLEDGMENTS

We gratefully acknowledge the efforts of Dr. G. T. Garvey and Dr. J. P. Schiffer in expediting the scheduling of the experiment at ANL. We further acknowledge the very fine beam preparation by both the ANL and BNL accelerator staffs. One of us (A.M.N.) would like to acknowledge several illuminating discussions about the data with Dr. P. Axel. We are indebted to Dr. J. Barrette for his critical reading of this manuscript. This work was supported in part by the National Science Foundation (NSF PHY77-27281), by a National Research Council of Canada Fellowship, and by the U. S. Department of Energy No. DE-AC02-76CH00016.

*Present address: Group P-3 MS 442, Los Alamos Scientific Lab, Los Alamos, New Mexico 87545.

[1]E. Almqvist, D. A. Bromley, and J. A. Kuehner, Phys. Rev. Lett. 4, 515 (1960).

[2]H. Feshbach, A. K. Kerman, and R. H. Lemmer, Ann. Phys. (N.Y.) 41, 230 (1967).

[3]H. Feshbach, J. Phys. (Paris) 37, C5 (1976).

[4]B. Imanishi, Nucl. Phys. A125, 33 (1969).

[5]J. Y. Park, W. Scheid, and W. Greiner, Phys. Rev. C 10, 967 (1974); J. Y. Park, W. Greiner, and W. Scheid, *ibid.* 16, 2276 (1977).

[6]G. I. Michaud and E. W. Vogt, Phys. Rev. C 5, 350 (1972).

[7]A. M. Sandorfi, L. R. Kilius, H. W. Lee, and A. E. Litherland, Phys. Rev. Lett. 40, 1248 (1978); see also A. M. Sandorfi, J. R. Calarco, R. E. Rand, and H. A. Schwettman, Phys. Rev. Lett. 45, 1615 (1980).

[8]A. M. Sandorfi and A. M. Nathan, Phys. Rev. Lett. 40, 1252 (1978).

[9]A. M. Sandorfi in *Clustering Aspects of Nuclear Structure and Nuclear Reactions (Winnepeg, 1978)* Proceedings of the 3rd International Conference on Clustering Aspects of Nuclear Structure and Nuclear Reactions, edited by W. T. H. van Oers, J. P. Svenne, J. S. C. McKee, and W. R. Falk (AIP, New York, 1978), p. 185.

[10]A. M. Nathan, T. J. Bowles, and A. M. Sandorfi, Bull. Am. Phys. Soc. 24, 666 (1979).

[11]A. M. Sandorfi and A. M. Nathan, Bull. Am. Phys. Soc. 25, 590 (1980).

[12]See, for example, M. D. Hasinoff, S. T. Lim, D. F. Measday, and T. J. Mulligan, Nucl. Instrum. Methods 117, 375 (1974).

[13]There are three absolute measurements of the $^{11}B(p,\gamma_0)^{12}C$ cross section available in the literature: (a) R. G. Allas, S. S. Hanna, L. Meyer-Schützmeister, and R. E. Segel, Nucl. Phys. 58, 122 (1964); (b) C. Brassard, H. D. Shay, J. P. Coffin, W. Scholz, and D. A. Bromley, Phys. Rev. C 6, 53 (1972); (c) M. Suffert, *Proceedings of the International Conference on Photonuclear Reactions and Applications, Asilomar 1973,* edited by B. L. Berman, p. 741. The last reference contains a renormalization of the excitation functions given in (a) and (b) based upon independent measurements at a few selected energies. The cross sections quoted in these publications differ by up to a factor of 2. The $^{11}B(p,\gamma_0)^{12}C$ cross section has been carefully remeasured with the BNL No. 2 detector [A. M. Sandorfi and M. T. Collins (unpublished)], and the value of $d\sigma/d\Omega_{lab}$ ($\theta_\gamma=90°$) = 7.7 μb/sr obtained at $Ep=6.00$ MeV has been used to normalize the efficiency-solid angle product for the $^{12}C(^{12}C,\gamma)^{24}$Mg measurements reported here. This value is in agreement with Ref. (c).

[14]M. H. Macfarlane and S. C. Pieper, Argonne National Laboratory (ANL) Report No. 76-11 (1978).
[15]W. Reilly, R. Wieland, A. Gobbi, M. W. Sachs, and D. A. Bromley, Nuovo Cimento 13A, 897 (1973).
[16]P. M. Endt and C. van der Leun, At. Data Nucl. Data Tables 13, 67 (1974).
[17]E. Almqvist, D. A. Bromley, J. A. Kuehner, and B. Whalen, Phys. Rev. 130, 1140 (1963).
[18]W. Galster, W. Treu, P. Dück, H. Fröhlich, and H. Voit, Phys. Rev. C 15, 950 (1977).
[19]S. K. Korotky, K. A. Erb, S. J. Willett, and D. A. Bromley, Phys. Rev. C 20, 1014 (1979).
[20]K. A. Erb, R. R. Betts, S. K. Korotky, M. M. Hindi, P. P. Tung, M. W. Sachs, S. J. Willett, and D. A. Bromley, Phys. Rev. C 22, 507 (1980).
[21]R. Wada, J. Schimizu, and K. Takimoto, Phys. Rev. Lett. 38, 1341 (1977).
[22]E. Kuhlmann, E. Ventura, J. R. Calarco, D. G. Mavis, and S. S. Hanna, Phys. Rev. C 11, 1525 (1975).
[23]R. Wada, T. Murakami, E. Takada, M. Fukada, and K. Takimoto, Phys. Rev. C 22, 557 (1980).
[24]A. Kiss, C. Mayer-Böricke, M. Rogge, P. Turek, and S. Wiktor, Phys. Rev. Lett. 37, 1188 (1976); D. H. Youngblood, C. M. Rozsa, J. M. Moss, D. R. Brown, and J. D. Bronson, Phys. Rev. C 15, 1644 (1977).
[25]F. E. Bertrand, K. van der Borg, A. G. Drentje, M. N. Harakeh, J. van der Plicht, and A. van der Woude, Phys. Rev. Lett. 40, 635 (1978); and K. van der Borg, Ph.D. thesis, Groningen, 1979 (unpublished).
[26]A. van der Woude in *Giant Multipole Resonances*, edited by F. E. Bertrand, Nuclear Science Research Conference Series (Harwood, Chur, 1979), Vol. 1, p. 65.
[27]H. Feshbach, C. E. Porter, and V. F. Weisskopf, Phys. Rev. 96, 448 (1954).
[28]A. M. Lane, Nucl. Phys. 11, 625 (1959).
[29]R. Stokstad, Yale Report No. 52 (1972) (unpublished).
[30]P. P. Singh, R. E. Malmin, M. High, and D. W. Devins, Phys. Rev. Lett. 23, 1124 (1969).
[31]L. Rosen, Helv. Phys. Acta, Exp. Suppl. 12, 253 (1966).
[32]F. Perey and B. Buck, Nucl. Phys. 32, 353 (1962).
[33]F. Ajzenberg-Selove, Nucl. Phys. A300, 1 (1978).
[34]P. M. Endt and C. van der Leun, Nucl. Phys. A310, 1 (1978).
[35]A. Gilbert and A. G. W. Cameron, Can. J. Phys. 43, 1446 (1965).
[36]P. E. Nemirovsky and Yu. V. Adamchuk, Nucl. Phys. 39, 551 (1962).
[37]T. Ericson, Adv. Phys. 9, 425 (1960).
[38]R. H. Lemmer and C. Toepffer, Phys. Rev. Lett. 44, 26 (1980).